

1 ***Quantifying the impact of lagged hydrological responses on the effectiveness of groundwater***
2 ***conservation***

3
4 **Authors:** Thomas J Glose¹, Samuel C Zipper¹, David W Hyndman^{2,3}, Anthony D Kendall³,
5 Jillian M Deines⁴, James J Butler, Jr.¹

6
7 **Affiliations:**

8 1. Kansas Geological Survey, University of Kansas, Lawrence KS, 66047, USA

9 2. School of Natural Sciences and Mathematics, University of Texas at Dallas, Richardson, TX,
10 75080, USA

11 3. Department of Earth and Environmental Sciences, Michigan State University, East Lansing,
12 MI, 48824, USA

13 4. Department of Earth System Science and Center on Food Security and the Environment,
14 Stanford University, Stanford, CA, 94035, USA

15
16 **Corresponding Author:** tomglose@ku.edu

17
18 **Author ORCID IDs:**

19 Glose: 0000-0002-5414-3571

20 Zipper: 0000-0002-8735-5757

21 Hyndman: 0000-0001-9464-8403

22 Kendall: 0000-0003-3914-9964

23 Deines: 0000-0002-4279-8765

24 Butler: 0000-0002-6682-266X

25
26 This is a non-peer-reviewed manuscript which has been submitted to *Water Resources Research*.

27
28 **Keywords:** numerical modeling, lagged processes, groundwater conservation, pumping
29 reductions, irrigation practices

30
31 **Key Points:**

- 32 • The long-term effectiveness of pumping reduction-based groundwater conservation is
33 dependent on lagged processes

34

35 **Abstract**

36 Many irrigated agricultural areas seek strategies to prolong the lifespan of their
37 groundwater resources. However, it is unclear how lagged responses, such as reduced
38 groundwater recharge caused by more efficient irrigation, may impact the ultimate effectiveness
39 of these initiatives. Here, we use a variably saturated groundwater model to: 1) analyze aquifer
40 responses to pumping reductions, 2) quantify time lags between reductions and water level
41 responses, and 3) identify the physical controls on lagged responses. We explore a range of
42 plausible model parameters for an area of the High Plains Aquifer (USA) where stakeholder-
43 driven conservation has slowed groundwater depletion. We identify two types of lagged
44 responses that reduce the long-term effectiveness of groundwater conservation. When vertical
45 hydraulic conductivity (K_z) is $> 3.5 \times 10^{-3} \text{ m d}^{-1}$, more efficient irrigation reduces groundwater
46 recharge on sub-decadal timescales (recharge-dominated response). By contrast, when K_z is $<$
47 $3.5 \times 10^{-3} \text{ m d}^{-1}$, changes in recharge are negligible, but pumping reductions alter the lateral flow
48 between the groundwater conservation area and the surrounding regions over decadal timescales
49 (lateral-flow-dominated response). For the modeled area, we found that a pumping reduction of
50 30% resulted in median usable lifetime extensions of 20 or 25 years, depending on the dominant
51 lagged response mechanism (recharge- vs. lateral-flow-dominated). These estimates are far
52 shorter than estimates made without accounting for the lagged responses. Our results indicate
53 that conservation-based pumping reductions can extend aquifer lifespans, but lagged responses
54 can create a sizable difference between the initial and long-term effectiveness of those
55 conservation measures.

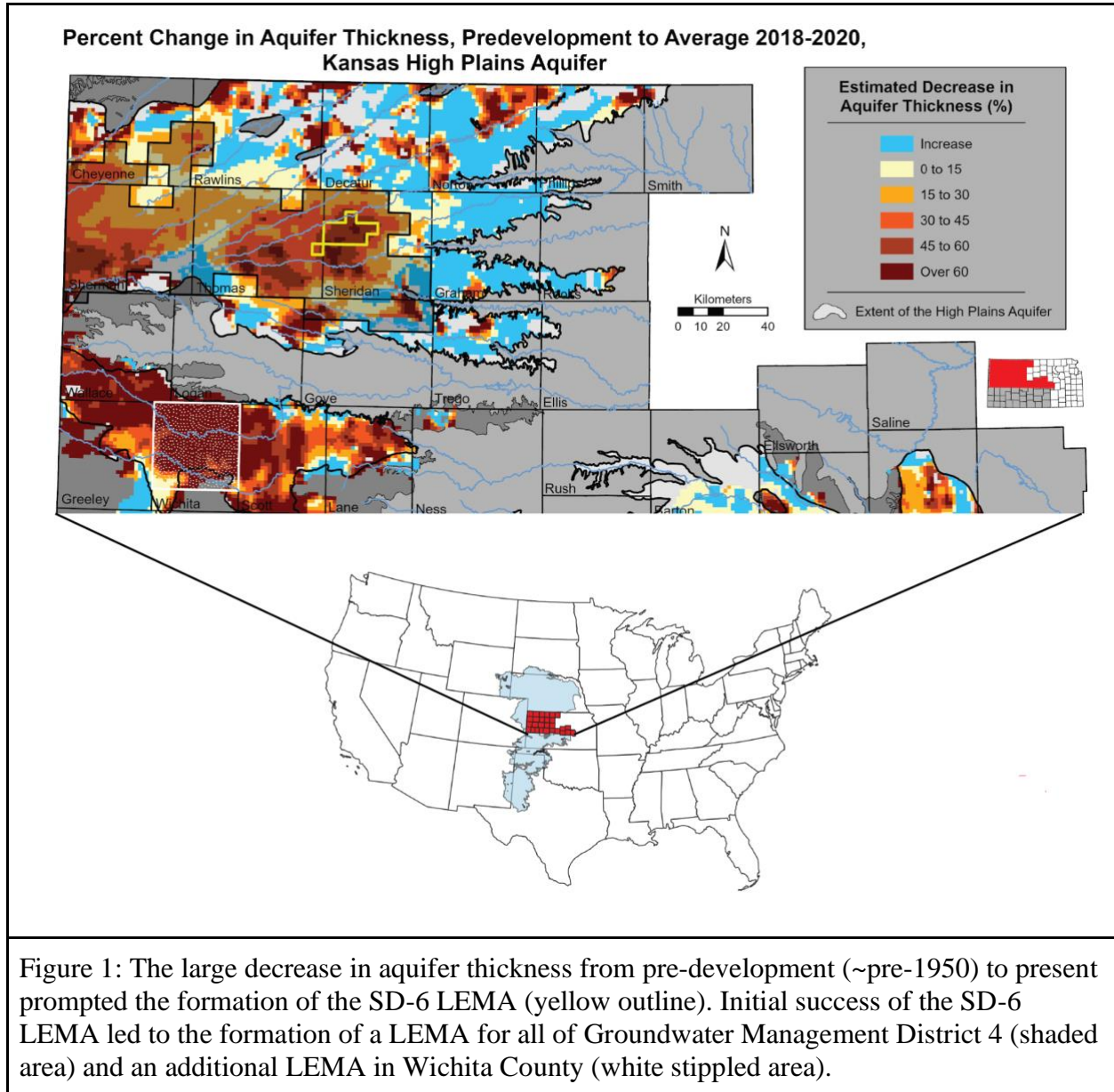
56 **1. Introduction**

57 Irrigation uses the majority (69%) of fresh groundwater withdrawals in the United States
58 (DeSimone et al., 2015; Dieter et al., 2018). In many aquifers supporting irrigated agriculture,
59 heavy pumping has resulted in unsustainable water-level declines, threatening the economy and
60 environment (Aeschbach-Hertig & Gleeson, 2012; Deines et al., 2020; Scanlon et al., 2012). As
61 groundwater is a limited resource, how to mitigate these declines to extend the usable lifetime of
62 heavily stressed aquifers is a pressing question (Bierkens & Wada, 2019; Butler et al., 2020a;
63 Castilla-Rho et al., 2019; Gleeson et al., 2020). In semi-arid environments with little access to
64 surface water, groundwater conservation programs that seek to reduce pumping are one of the
65 only viable options to decrease groundwater declines in the near to moderate term (Butler et al.,
66 2020b; Deines et al., 2019; Hu et al., 2010).

67 One such program is Kansas' Local Enhanced Management Area (LEMA) program that
68 was recently implemented in several areas of the state (Figure 1). LEMAs are a stakeholder-
69 driven governance approach in which groundwater users (primarily irrigators) and groundwater
70 management districts develop conservation plans that are subsequently approved and enforced
71 by the state regulatory agency (Kansas Statutes Annotated 82a-1041, 2012). The state's first
72 LEMA, referred to as Sheridan-6 (SD-6), was initiated in 2013 in a 256-km² area in northwest
73 Kansas with the stated goal of reducing average annual pumping by 20% over a five-year period.
74 During this period, irrigators exceeded their goal, reducing pumping by 31% on average and
75 slowing water table decline rates while maintaining similar economic returns (Deines et al.,
76 2019, 2021; Golden, 2018). This initial success led to an extension of the SD-6 LEMA for an
77 additional five years, the 2018 formation of a much larger LEMA that encompasses most of the
78 northwest Kansas portion of the High Plains aquifer (Groundwater Management District 4), and

79 an additional 2021-initiated LEMA in west-central Kansas (Kansas Department of Agriculture,
80 2013, 2018, 2021) (Figure 1).

81



82

83 While initial results from the SD-6 LEMA are promising, it is not clear how the
84 effectiveness of such conservation initiatives might change in the future as the hydrological
85 system adjusts to the observed pumping reductions (Butler et al., 2020b; Deines et al., 2021;

86 Foster et al., 2017). The change in aquifer water levels in response to pumping is a function of
87 the difference between pumping and net inflow, which is defined as total inflows (i.e., recharge,
88 lateral inflows) minus all non-pumping outflows (i.e., discharge to streams, vegetation, lateral
89 outflows), and is mediated by hydrostratigraphic characteristics (Butler et al., 2016). However,
90 the relative contributions of vertical and lateral flows to net inflow are poorly understood (Butler
91 et al., 2016, 2020b). While recent work has found that reductions in aquifer net inflow can
92 decrease the effectiveness of groundwater conservation programs over time (Butler et al.,
93 2020b), it is highly uncertain how the mechanisms, timescales, and magnitudes of lagged
94 responses from different water balance components vary. For example, estimates of the
95 magnitude and transit time for groundwater recharge vary dramatically over the HPA due to
96 thick unsaturated zones (Gurdak et al., 2008; Katz et al., 2016; McMahon et al., 2006; Zell &
97 Sanford, 2020). As a result, we do not know which lagged responses may impact overall
98 groundwater sustainability, nor the timescales and controlling processes.

99 To address this knowledge gap, we seek to answer the question: *How do lagged*
100 *responses to pumping reductions impact the effectiveness of groundwater conservation practices*
101 *over time?* We hypothesize that when groundwater conservation initiatives, such as Kansas'
102 LEMA program, are enacted, (i) the reduction in pumping causes an immediate change to the
103 aquifer water balance, leading to a slowing of the water table decline rate (Figure 2a, light blue
104 line); (ii) over time, inflows will diminish because the reduction in deep percolation (water that
105 drains below the rooting zone) associated with more efficient irrigation (Deines et al., 2021) will
106 eventually reduce recharge to the aquifer. Similarly, lateral inflow to the conservation area will
107 diminish, as decreased pumping will reduce the hydraulic gradient driving water into the area. In
108 both situations, the result will be an increase in water table declines to an intermediate rate

109 between the pre-conservation decline rate and the immediate post-conservation rate (dark blue
110 line in Figure 2a). To test these hypotheses, we developed a variably saturated groundwater flow
111 model for the SD-6 LEMA based on historical observations and realistic conditions. We used
112 this model to evaluate the long-term changes in the aquifer water balance associated with
113 groundwater conservation, quantify the implications of lagged responses for estimates of usable
114 aquifer lifetimes, and determine the physical controls on these lagged responses.

115 **2. Methods**

116 *2.1 Model Overview*

117 To test our hypotheses, we developed a representative variably saturated groundwater
118 flow model of a north-south linear transect that passes through the SD-6 LEMA (Figure 2b). We
119 elected to build a simplified model, rather than a fully-calibrated three-dimensional groundwater
120 flow model, to better isolate the hydrological processes of interest, and more directly test our
121 hypotheses by avoiding unnecessary site-specific complexity--an approach known as surrogate
122 or archetypal modeling (Asher et al., 2015; Razavi et al., 2012; Voss, 2011a, 2011b; Zipper et
123 al., 2018, 2019). Nevertheless, to ensure our model provided a reasonable simulation of the
124 dominant processes in this region, we conducted an evaluation against field data from the SD-6
125 region.

126 *2.2 Model Construction and Input Data*

127 We used the United States Geological Survey's MODFLOW-NWT program and
128 constructed the model using the Python package FloPy (Bakker et al., 2016). The 40 km long
129 domain consists of a single layer of 50 grid cells, each 800 m by 800 m in size, covering a total
130 area of 32 km². Each grid cell is roughly equivalent in area to an average quarter-section field
131 (64.75 hectares [160 acres]) and cell dimensions were set based on the average distance between

132 irrigation wells in the area. The model domain was split into two types of management practices
133 (conservation and non-conservation; blue and orange areas, respectively, in Figure 2b), which
134 were represented in the model using different pumping and deep percolation rates as described
135 below. The conservation area was made up of 14 grid cells while the non-conservation areas
136 each consisted of 18 grid cells to remove the influence of edge effects from the northern and
137 southern no-flow boundaries. The single model layer is 72 m thick and starting pressure heads
138 were set to 40 m; these values represent the average depth to bedrock and pressure heads,
139 respectively, of the area for the pre-development period (~pre-1950) (Fross et al., 2012). The top
140 of the model is assumed to be below the rooting zone to remove the influence of
141 evapotranspiration, overland flow, and discharge to surface water bodies. Since regional
142 groundwater flow is generally from west to east (perpendicular to our transect), we included a
143 lateral flow boundary condition on the west side and a no-flow boundary on the east to represent
144 the net lateral flow entering the SD-6 LEMA, which is distinct from the vertical inflow from
145 groundwater recharge. We varied net lateral flows along with the model hydrostratigraphic
146 properties as described in Section 2.3.

147 Pumping is simulated using MODFLOW's well (WEL) package. We estimated annual
148 pumping volumes by establishing relationships between annual precipitation depth and measured
149 pumping during the 2000-2018 period (Figure 3), when a large majority of irrigators had
150 transitioned from traditional high pressure center pivot irrigation to more efficient center pivot
151 with drop nozzle irrigation (Pfeiffer & Lin, 2010; Rogers & Lamm, 2012). We first estimated a
152 relationship between precipitation and pumping for the "No Conservation" portions of the
153 domain that included the period after the establishment of the SD-6 LEMA; observed pumping
154 rates from the SD-6 LEMA were translated upward to account for the climate-adjusted average

155 27% reduction in pumped volume observed during the first four years of the LEMA (Whittemore
156 et al., 2018). Using the “No Conservation” relationship as the baseline, two additional
157 relationships were developed for the pumping scenarios modeled in this study (Figure 3a): (i) a
158 20% pumping reduction scenario based on the legal requirements for the SD-6 LEMA; and (ii) a
159 30% pumping reduction scenario that more closely reflects observed irrigator behavior. For each
160 pumping scenario, we applied the estimated annual pumping volume uniformly over a 103-day
161 period, which was the average time between the onset and cessation of irrigation pumping as
162 observed in high temporal-resolution well observations (Butler et al., 2019). The applied
163 pumping volume was computed as the area of a single grid cell times the irrigation depth from
164 the statistical relationship established in Figure 3a. As discussed in Section 2.1, our surrogate
165 modeling approach is not intended to precisely represent observed spatial pumping dynamics
166 within the SD-6 LEMA, but rather the average aquifer response to typical regional pumping. To
167 reflect that the estimated pumping volume is representative of the entire SD-6 area, which is
168 heavily irrigated, we placed a pumping well in each individual grid cell both inside and outside
169 the conservation area.

170 The model simulates flow through variably saturated porous media using the unsaturated
171 zone flow (UZF) package, which uses a kinematic-wave approximation to solve the 1-D
172 Richard’s equation (Niswonger et al., 2006; Smith, 1983; Smith & Hebbert, 1983). While
173 numerous models can simulate variably saturated flow, the UZF package for MODFLOW has
174 several advantages for our purposes, including documented use in thick vadose zones (Hunt et
175 al., 2008; Nazarieh et al., 2018), computational efficiency (Kennedy et al., 2016; Niswonger &
176 Prudic, 2009), and widespread use (Bailey et al., 2013; Hou et al., 2020; Morway et al., 2013).
177 Since the top of our model domain represents the bottom of the root zone, we provided UZF with

178 annual values of deep percolation from a linear model fit between simulated deep percolation
 179 from a calibrated crop model for the SD-6 area with and without conservation (Deines et al.,
 180 2021), and the sum of annual precipitation and applied irrigation depth following Scanlon et al.
 181 (2006) (Figure 3b). Like pumping, annual deep percolation values were uniformly disaggregated
 182 to daily values over the 103-day pumping period. This assumption is justified because essentially
 183 all deep percolation in the area is the result of excess applied irrigation water (Ajaz et al., 2020).
 184 Unlike the separate relationships required for pumping under each conservation scenario, only
 185 one relationship is needed to estimate deep percolation because the effects of groundwater
 186 conservation are accounted for in the annual irrigation depth term. These relationships (Figures
 187 3a and 3b) were used to generate deep percolation rate time series data for both the evaluation
 188 and projection periods and pumping rate time series for the projection period (Figure 3c).

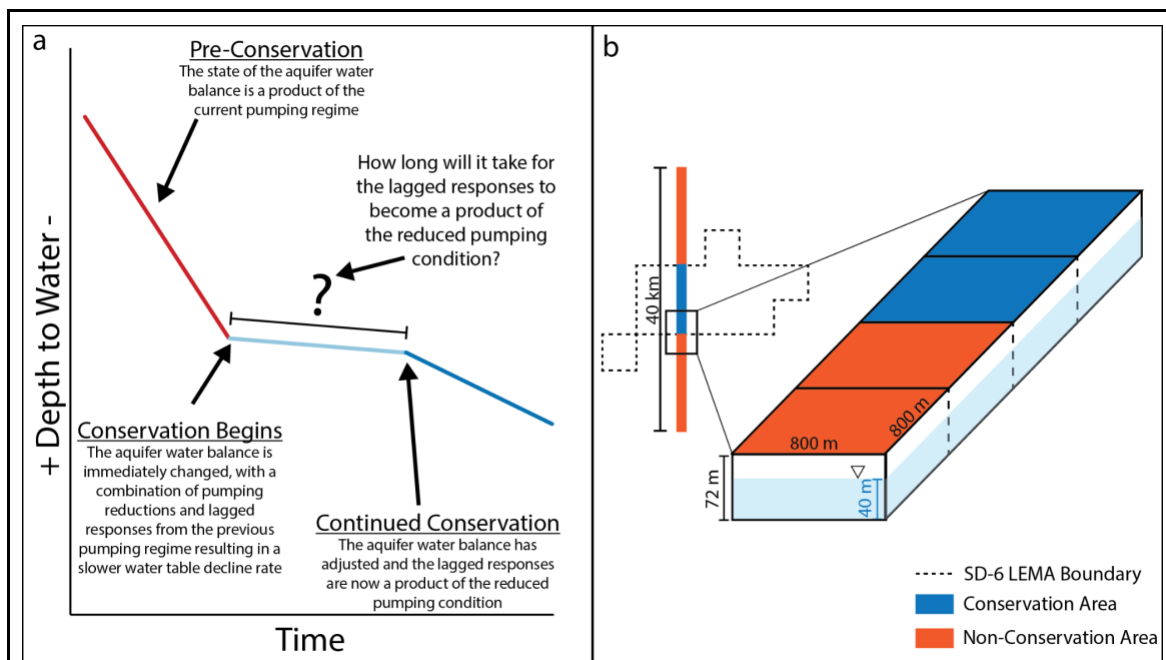


Figure 2: Conceptual diagrams. a) Graphical representation of how the aquifer water balance changes due to pumping reductions. The initial reduction in pumping causes an immediate change to the aquifer water balance, resulting from an initial period of high effectiveness (light blue line) that wanes in time as lagged responses, such as groundwater recharge and lateral flow, adjust to the new pumping regime (dark blue

line). b) Model overview, including the location of the transect relative to the SD-6 LEMA, the two separate areas (conservation and non-conservation), the grid cell dimensions, the domain depth, and the starting head value representative of the pre-development period.

189 Our simulations spanned 201 years (1900-2100), which can be divided into three periods:
190 spin-up (1900-1954), historical (1955-2019), and projection (2020-2100). The 55 year spin-up
191 period is prior to the onset of high capacity pumping in the region so the only fluxes in/out of the
192 domain are deep percolation, which was applied at a rate of $5 \times 10^{-4} \text{ m d}^{-1}$ ($\sim 51 \text{ mm yr}^{-1}$) to
193 approximate pre-development recharge in the area (Fross et al., 2012; Hansen, 1991), and the
194 applied lateral inflows. To ensure that recharge and lateral inflow did not change the prescribed
195 pre-development saturated zone pressure heads, a drain was placed at the pre-development water
196 level (40 m) across the domain. This approximates the effect of the regional streams that drained
197 the system during the pre-development period. After the spin up period, a mix of regression-
198 estimated (1955 to 1992) (Wilson et al., 2005) and measured pumping volumes (1993 to 2019)
199 for the SD-6 area was used to generate normalized pumping rates which were applied to the
200 model (Figure 3c). As observed irrigator behavior within the LEMA was close to the 30%
201 pumping reduction scenario, we used the 30% reduction pumping rates for 2013-2019. The
202 projection period (2020-2100) allows us to evaluate the long-term implications of pumping with
203 the baseline and the two reduction (20% and 30%) pumping scenarios. For the projection period,
204 we randomly sampled annual precipitation from the historical precipitation record to estimate
205 pumping and deep percolation for each year based on the relationships shown in Figure 3 since
206 there are no consistent long-term historical (Lin et al., 2017) or projected (Figure S1)
207 precipitation trends in this region, and historical precipitation patterns do not exhibit significant
208 temporal autocorrelation (Butler et al., 2020).

209 **2.3 Model Evaluation and Sensitivity Analysis**

210 We used a Latin hypercube sampling scheme (McKay et al., 1979) to identify the model
 211 parameters that best reproduced observed hydrological data and evaluate the sensitivity of model
 212 output to each parameter and the interactions between parameters (Zipper et al., 2018). Our Latin
 213 hypercube sample consisted of 2,000 near-random, unique sets of hydrostratigraphic parameters
 214 (vertical saturated hydraulic conductivity, K_z ; specific yield, S_Y ; Brooks and Corey epsilon, ϵ)
 215 and lateral inflow (LI), which were selected from a uniform distribution over the parameter space
 216 shown in Table 1. We ran one simulation using each parameter set to explore lagged responses to
 217 groundwater conservation across a range of hydrogeological settings and to reduce the risk of
 218 identifying a local optima as the best parameter set.

Table 1: Parameter space ranges for the Latin hypercube sampling scheme. As we are taking a surrogate modeling approach, ranges were extended outside of their observed values for the area to allow the parameter space to be fully explored. ¹(Fross et al., 2012) · ²(Butler et al., 2016), ³(Brooks & Corey, 1966)

Parameter	Lower Bound	Upper Bound
\log_{10} Vertical Hydraulic Conductivity (m d^{-1})^[1]	-6	1
Specific Yield (-)^[2]	0.06	0.18
Brooks and Corey Epsilon (-)^[3]	2	5
\log_{10} Lateral Inflows (m d^{-1})^[2]	-6	-3

219
 220 Horizontal hydraulic conductivity and saturated water content were held constant at 20 m
 221 d^{-1} and 0.25, respectively, to reflect average values in the SD-6 LEMA area (Fross et al., 2012).
 222 The UZF package relies on the Brooks and Corey function to calculate unsaturated K_z (Brooks

223 & Corey, 1966). This function requires residual water content, here approximated for each
224 parameter set by taking the S_Y value for each set and subtracting it from the saturated water
225 content (Niswonger et al., 2006). A value of 0.005 was added to the calculated residual water
226 content to ensure that the unsaturated hydraulic conductivity value did not start at a value of
227 zero.

228 We evaluated the performance of each of the 2000 simulations via comparison to the
229 observed groundwater level data for the 1999-2019 period, which represents the longest
230 continuous record of reliable observations within the SD-6 LEMA (KGS WIZARD Database;
231 <http://www.kgs.ku.edu/Magellan/WaterLevels/index.html>). The goal of this study is to ensure
232 that the dominant processes (e.g., pumping reductions and lagged responses) are appropriately
233 simulated while not overparameterizing the model since our focus is not on site-specific
234 heterogeneity (Konikow & Bredehoeft, 1992).

235 We quantified model performance for each parameter set using a two-step approach.
236 First, as the area has experienced significant drawdown, we eliminated model runs in which the
237 head in the model domain at the end of the historical period (2019) was still at pre-development
238 levels (Fross et al., 2012). For the remaining runs, we calculated the Kling-Gupta Efficiency
239 (KGE; Kling et al., 2012) score for both the annual water table elevation and the interannual
240 change in water table elevation, which are based on measurements taken each January in the
241 LEMA area. We selected these two metrics to ensure that both the interannual and long-term
242 dynamics were simulated reasonably, and used the minimum (lower-performing) of these two
243 KGE values as the final KGE score for that parameter set. We then divided the model runs into
244 four performance groups: poor ($KGE < -0.41$, which indicates that the model results are worse
245 than the mean of the observations; Knoben et al., 2019), low ($-0.41 < KGE < 0$), medium ($0 <$

246 KGE < 0.5), and high (KGE > 0.5). A KGE score of 1 would indicate a perfect match between a
247 simulation and observations. Only runs in the high performance group were analyzed for the
248 projection period because those parameter sets were judged able to reasonably approximate
249 historical hydrological conditions.

250 The models selected for projection were run to the year 2100 and the extension of the
251 usable aquifer lifetime was quantified for the 20% and 30% pumping reduction scenarios. For
252 each parameter combination and pumping scenario, the extension of the usable aquifer lifetime is
253 calculated as the number of years that water levels in the aquifer remain above a minimum
254 threshold relative to the baseline “No Conservation” scenario. For this region, we assumed that a
255 minimum saturated thickness of eight meters is required for large-scale irrigation to allow for
256 sufficient transmissivity, and therefore well yield, along with pumping-induced drawdown in the
257 well (Butler et al., 2020b).

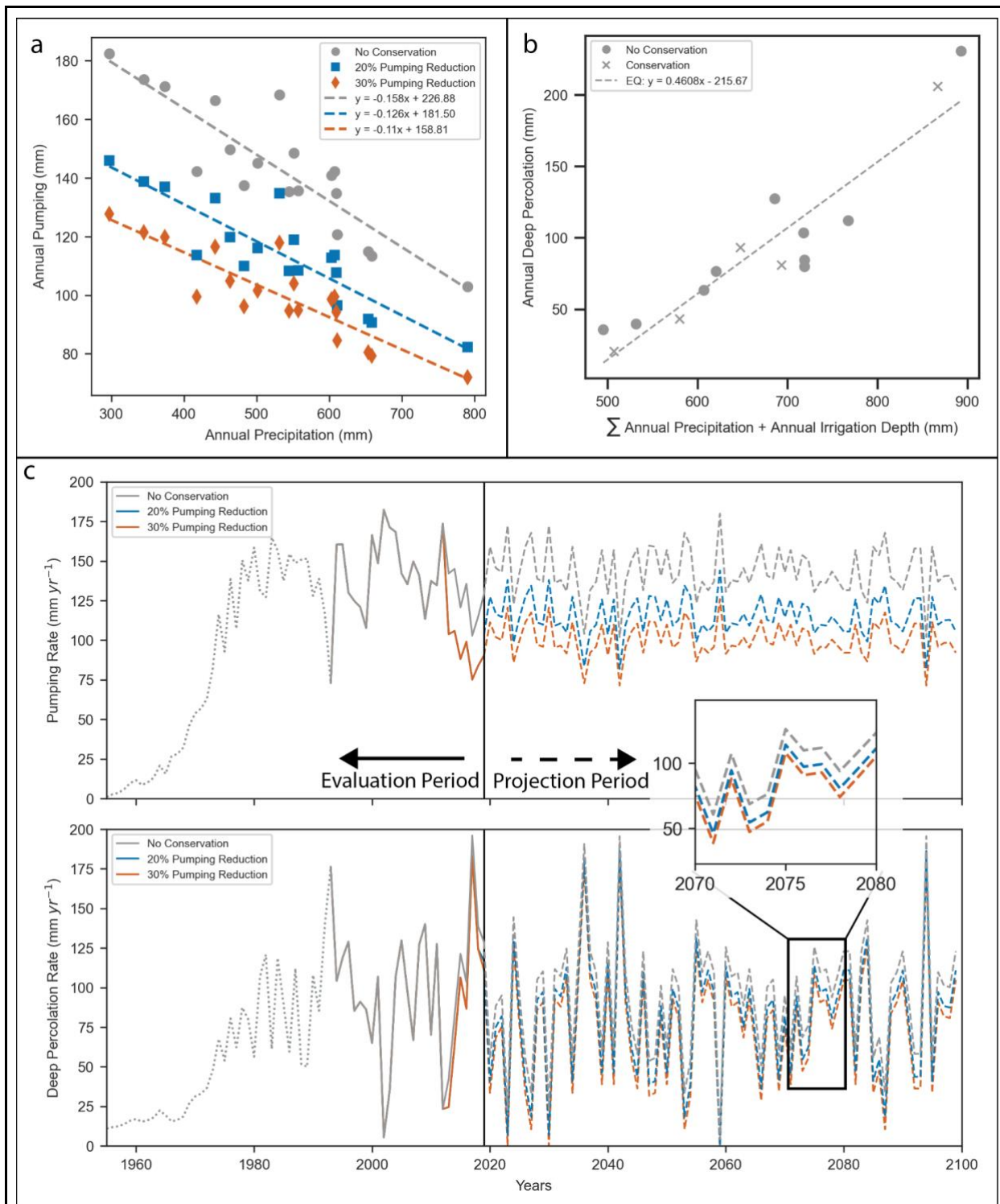


Figure 3: Annual statistical relationships for: a) pumping depth, b) deep percolation depth, and resulting applied c) pumping rate and d) deep percolation from the statistical relationships. For three very dry years in the prediction period, the statistical relationship in panel b produced negative deep percolation rates; these years were assigned a rate of 0 m d^{-1} . For the historical

period, pumping rate and deep percolation are shown only for the 30% pumping reduction scenario (orange) as this best represents observed irrigator behavior.

258 **3. Results and Discussion**

259 **3.1 Recharge and lateral flow-dominated inflows**

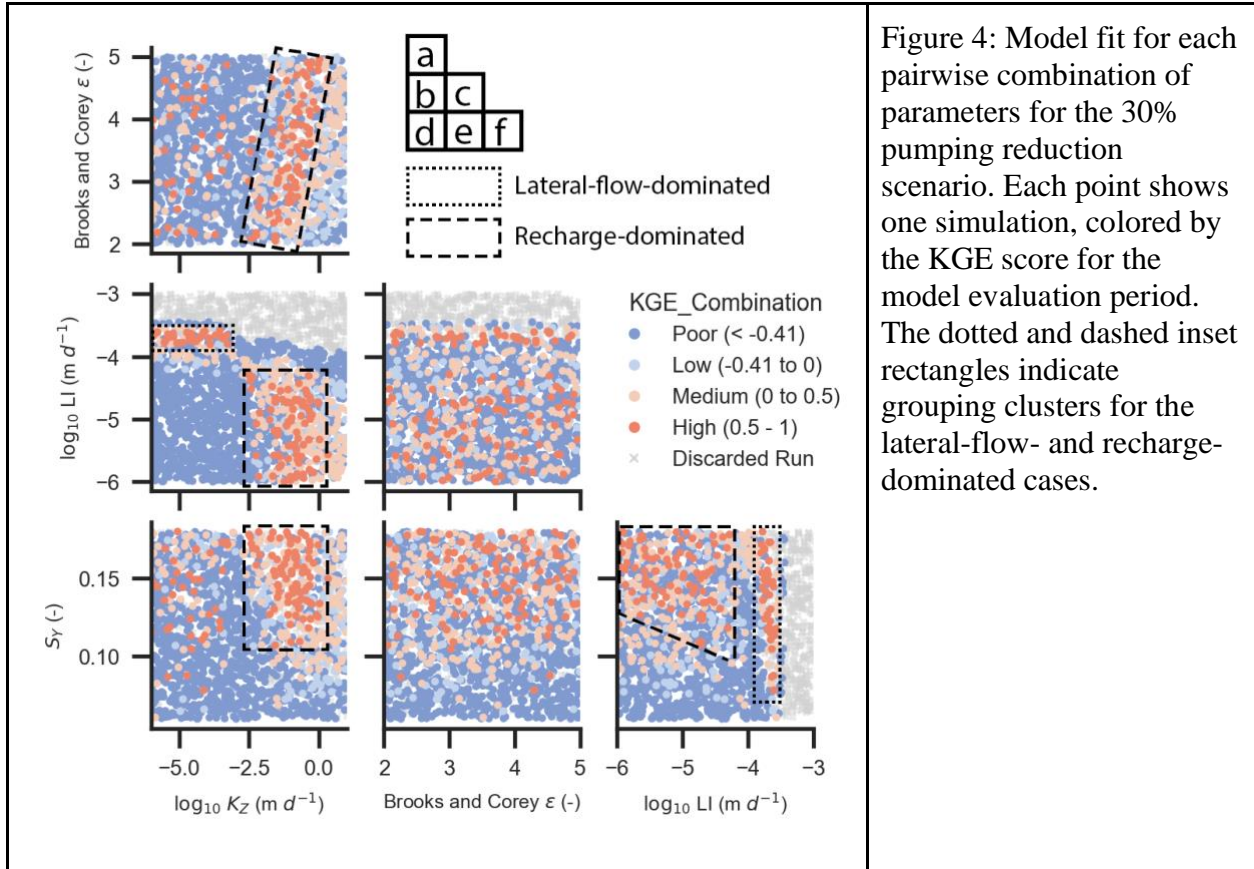


Figure 4: Model fit for each pairwise combination of parameters for the 30% pumping reduction scenario. Each point shows one simulation, colored by the KGE score for the model evaluation period. The dotted and dashed inset rectangles indicate grouping clusters for the lateral-flow- and recharge-dominated cases.

260 We found that many parameter combinations were able to reproduce the historical head
 261 and head change observations (Figure 4). Of the 2,000 parameter combinations tested, there were
 262 121 simulations with high performance (Figure 4, dark red circles, $KGE > 0.5$). An additional
 263 206 were rated as medium, 127 as low, 1,098 as poor, and 448 were discarded due to no
 264 simulated drawdown (Figure 4). Within parameter pairs, there are several clusters that occur
 265 throughout the parameter space (Figure 4b), the most evident occurring between lateral inflow
 266 (LI) and vertical hydraulic conductivity (K_z). In parameter space, these two clusters correspond
 267 to a high LI/low K_z zone, in which lateral groundwater flow is the dominant inflow to the

268 aquifer, and a low LI/high K_z zone, in which vertical groundwater recharge is the dominant
269 inflow to the aquifer .

270 For the lateral-flow-dominated case, the parameter sets that yield high KGE scores have
271 LI values between 1.6×10^{-4} and $2.5 \times 10^{-4} \text{ m d}^{-1}$ and K_z values between 1×10^{-6} (the lower
272 bound of the parameter space tested) and $5 \times 10^{-4} \text{ m d}^{-1}$. However, for the Brooks and Corey ϵ
273 and S_Y there are no clear thresholds, indicating that the rate of lateral flow is the controlling
274 factor. The ranges of K_z and LI values with good fits in the recharge-dominated case are
275 opposite of the lateral-flow-dominated case, with higher K_z values (from 3.5×10^{-3} to 1 m d^{-1})
276 and lower LI values (from $5 \times 10^{-5} \text{ m d}^{-1}$ to the lower bound of the parameter space tested, 1×10^{-6}
277 m d^{-1}) (Figure 4b). In contrast to the lateral-flow-dominated case, the recharge-dominated case
278 is also sensitive to the Brooks and Corey ϵ and S_Y . As K_z approaches 1 m d^{-1} , the value of ϵ
279 steadily increases from 2 to 5 (Figure 4a). The range of S_Y is also limited based on K_z , with S_Y
280 values between 0.1 and 0.18 necessary to generate KGE scores of ≥ 0.5 (Figure 4d). Vertical
281 hydraulic conductivity is not the only controlling factor in the recharge-dominated case. As the
282 value of LI increases towards its upper limit of $5 \times 10^{-5} \text{ m d}^{-1}$, the range of S_Y also expands with
283 its lower limit dropping from 0.13 to 0.1 (Figure 4f). The interplay between hydrostratigraphic
284 parameters plays a more prominent role in the recharge-dominated scenario. Along with K_z , the
285 Brooks and Corey ϵ and S_Y influence the rate and volume of vertical water movement through
286 the thick vadose zone, respectively, and therefore influence the performance of the model.

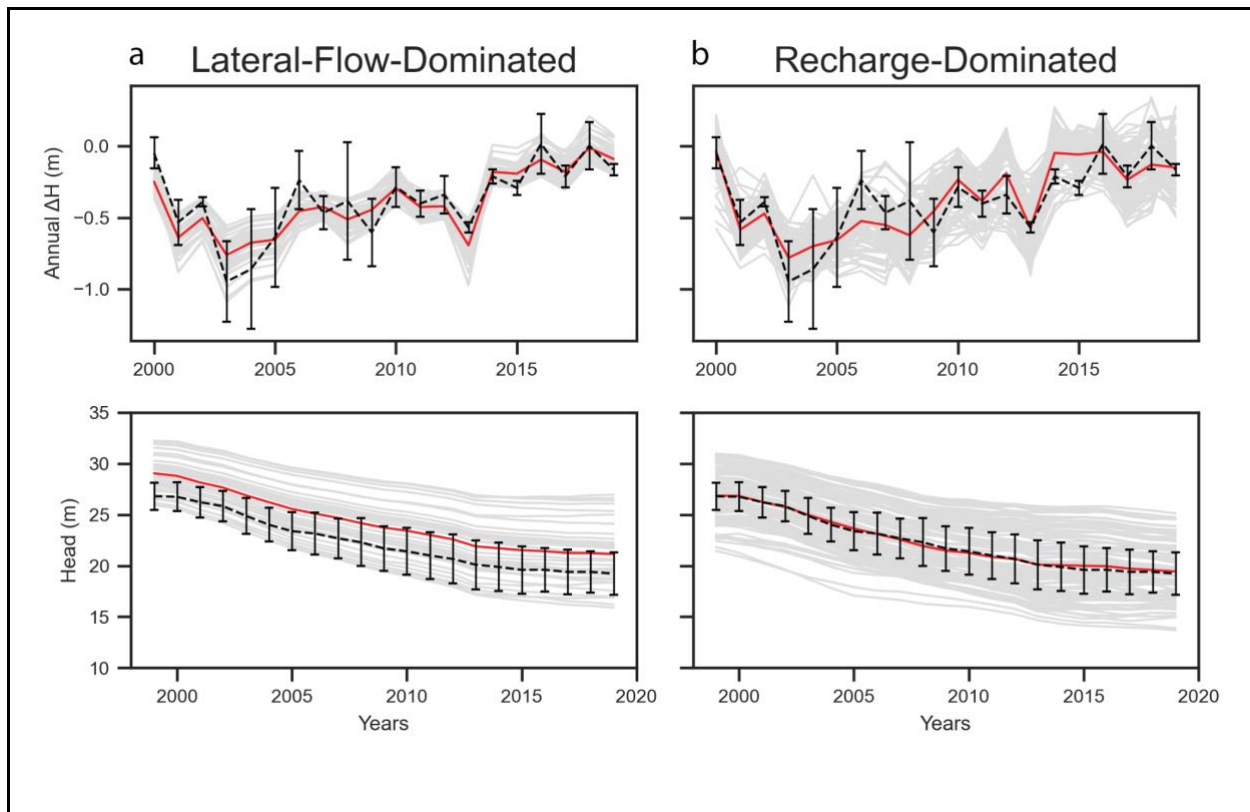


Figure 5: Results for the 30% pumping reduction scenario of observed (black, dashed line), simulated (light gray, solid lines), and average simulated (red lines) interannual change in pressure head and annual pressure head values for the a) lateral-flow-dominated and b) recharge-dominated cases. Simulation results presented for the center cell in the conservation area, the error bars show one standard deviation about the mean of the observed data.

287

288 For both the lateral-flow-dominated and recharge-dominated cases, the average simulated

289 interannual change in pressure head and annual pressure head values (Figure 5a, b, red lines)

290 closely align to the average observed value (Figure 5a, b, dashed lines). The individual

291 components of the KGE score (mean Pearson correlation coefficient, variability ratio, and bias

292 ratio; (Kling et al., 2012)), KGE score, and root mean square error (RMSE) for all high-

293 performing recharge- and lateral-flow-dominated cases are given in Table 2 for the 1999-2019

294 evaluation period. The average simulated values also fell within or close to the standard

295 deviation of the observed measurements, indicating that the model is reasonably capturing the

296 annual and interannual dynamics of the natural system.

Table 2: Average model statistics for interannual and annual heads for the lateral-flow-dominated and recharge-dominated cases.

Statistic	Lateral-Flow-Dominated		Recharge-Dominated	
	Interannual Change in Head	Annual Head	Interannual Change in Head	Annual Head
Pearson Correlation Coefficient (r)	0.887	0.998	0.732	0.993
Variability Ratio (γ)	0.838	0.999	1.139	1.042
Bias Ratio (β)	1.044	1.056	0.982	0.973
Kling Gupta Efficiency Score (KGE)	0.685	0.765	0.643	0.762
Root Mean Square Error (m) (RMSE)	0.142	2.269	0.204	2.529

297 The wide variety of parameters that lead to reasonable agreement with the observed data
 298 indicates that multiple interpretations of the underlying processes that dictate groundwater
 299 recharge in areas with thick vadose zones are equally valid, following the principle of
 300 equifinality (Beven, 2006). In groundwater modeling, parameter estimation often seeks to find a
 301 local or global optimum to match limited observations while minimizing an objective function
 302 using software such as PEST (Doherty, 2015) or UCODE (Poeter & Hill, 1999). However, the
 303 hunt for an ideal parameter set that results in simulated values closely matching observed values
 304 can ignore other possible parameter sets that perform nearly equally well (Savenije, 2001). This
 305 is true for our surrogate model of the SD-6 area as the lack of vadose zone observation data
 306 paired with an exploration of a wide parameter space resulted in two possible and equally valid
 307 mechanisms that affect the long term performance of pumping reduction-based groundwater
 308 conservation initiatives.

309 ***3.2 Lagged responses to conservation in recharge- and lateral flow-dominated conditions***

310 Due to differences in their underlying hydrological processes, recharge-dominated and
311 lateral-flow-dominated cases exhibit different long-term hydrological responses to groundwater
312 conservation. In lateral-flow-dominated settings, changes in deep percolation caused by pumping
313 reductions do not significantly impact recharge rates within the 80-year projection period
314 because recharge rates are low to begin with and changes in deep percolation take a long time to
315 propagate down to the water table (Figure 6a). Following reductions in pumping, water table
316 decline rates are initially sizably reduced then increase through time, consistent with our
317 hypothesis (Figure 2a). The increase occurs because the initial reduction within the conservation
318 area creates a lateral hydraulic gradient that drives lateral flow into the surrounding non-
319 conservation area; this phenomenon is further discussed in Section 3.3. The lateral flow-
320 dominated case relies on high fluxes of net lateral inflow to compensate for the lack of recharge.
321 This case only applies when K_z values are low as any increase in recharge would add too much
322 water to the aquifer, resulting in unrealistic rises in the water table. When LI is the controlling
323 mechanism, the vadose zone properties have a negligible impact on the effectiveness of the
324 pumping reductions.

325 In recharge-dominated cases, the rate of deep percolation eventually controls the rate of
326 groundwater recharge. Reductions in pumping decrease the amount of water that is applied in
327 excess of crop water demands, and thus reduce the rate of deep percolation (Figure 3b). Unlike
328 the lateral flow-dominated case where there is no difference in recharge between the
329 conservation and non-conservation areas, the effects of changing deep percolation lead to a
330 reduction in groundwater recharge within the conservation area relative to the non-conservation
331 area (Figure 6b). Once the lagged response of recharge adjusts to the reduced pumping condition,

332 water table decline rates increase, consistent with our hypothesis. However, even in recharge-
333 dominated settings, the effects of changing lateral outflows still play an important role. Lateral
334 outflows across the border of the conservation area reach up to $\sim 25 \text{ mm yr}^{-1}$, which is
335 comparable to the difference in recharge between the conservation and non-conservation areas
336 (Figure 6b).
337

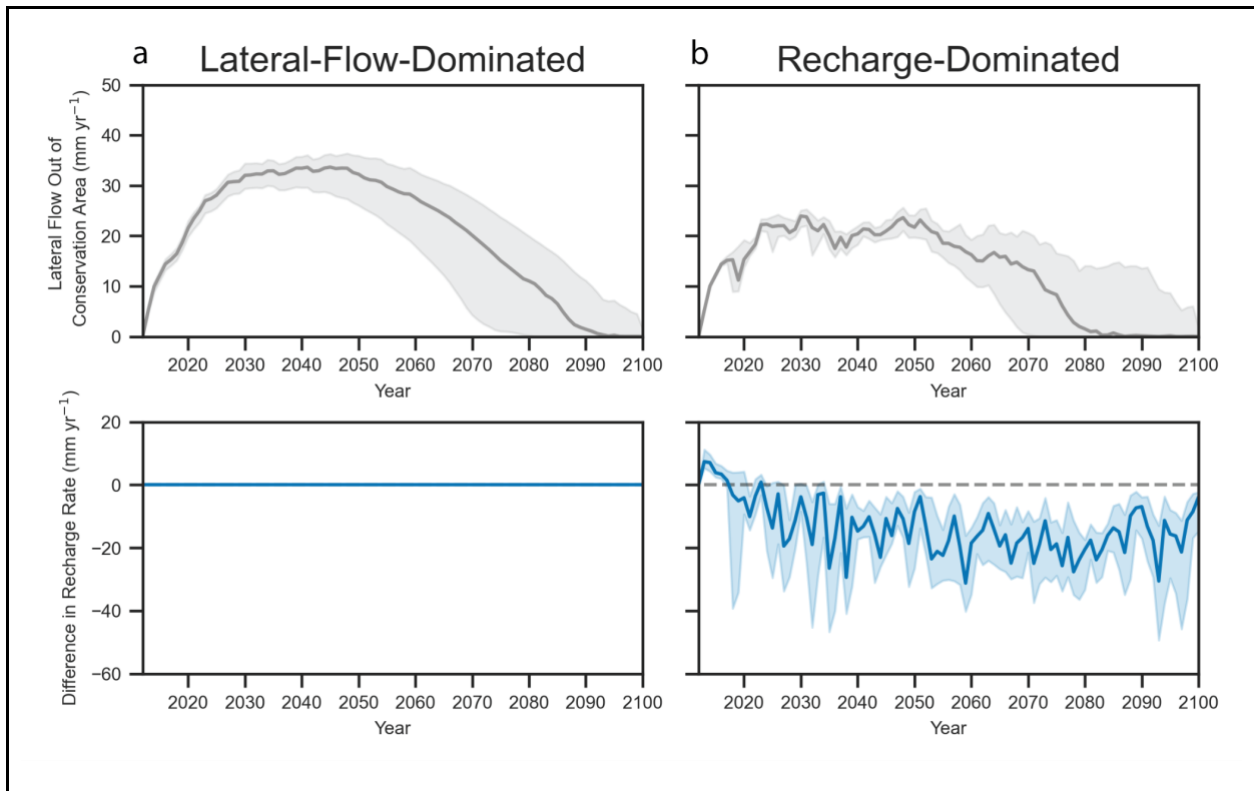


Figure 6: Average time series of simulated lateral outflow from the conservation area to the non-conservation area (upper plots) and difference in recharge rate between the conservation area and the non-conservation area (lower plots) for a) the lateral-flow-dominated and b) recharge-dominated cases. Thick lines represent average values across all model runs used for the projections and the shading indicates the interquartile range.

338
339 These two processes have distinct time lags from the onset of groundwater conservation
340 measures. For the lateral-flow-dominated cases, flow out of the conservation area begins with the
341 start of pumping reductions and increases quickly with the development of a head gradient

342 between the conservation and non-conservation areas. Eventually, lateral outflow peaks at a rate
343 of $\sim 34 \text{ mm yr}^{-1}$ from 2030 to 2050, or ~ 17 to ~ 37 years after the onset of conservation (Figure
344 6a). After 2050, lateral outflow gradually decreases due to a decline in the head gradient between
345 the conservation and non-conservation areas, typically reaching 0 mm yr^{-1} between 2080 and
346 2100 depending on the case. In the recharge-dominated cases (Figure 6b), lateral flow out of the
347 conservation area follows a similar pattern, though with a lower peak ($\sim 24 \text{ mm yr}^{-1}$) and more
348 interannual variability. The interannual variability in lateral outflows in the recharge-dominated
349 cases is due to differences in recharge rates between the conservation and non-conservation
350 areas, with larger lateral outflows when the recharge differences between the conservation and
351 non-conservation areas are greater because this induces a larger hydraulic gradient between the
352 two areas. For the recharge-dominated cases, there is an immediate short lived-period of positive
353 differences in recharge rates, with recharge into the conservation area greater than into the non-
354 conservation area because the reduction in water table decline rates allows more recharge to
355 reach the water table than at higher decline rates. After five years, recharge rates in the
356 groundwater conservation area adjust to the lower deep percolation rates associated with the
357 reduced pumping condition, resulting in a negative difference for the rest of the simulation.

358 These differences between the lateral- and recharge-dominated cases indicate that, in
359 settings with higher values of K_z ($> 0.0035 \text{ m d}^{-1}$; Figure 4), excess applied irrigation water can
360 traverse the thick vadose zone that is present in western Kansas and ultimately recharge the
361 water table. However, vertical hydraulic conductivity is not the only controlling factor in the
362 recharge-dominated cases, as LI , S_Y , and Brooks and Corey ϵ also play important roles in the
363 long-term effectiveness (see Figure 4). In cases where S_Y is low, high-performing parameter sets
364 tend to have a greater LI to compensate for the low drainable pore space. When K_z values are

365 low, Brooks and Corey ϵ values must be low as well to allow for the calculated unsaturated
366 hydraulic conductivity value to be high enough to transmit water through the vadose zone at a
367 rapid enough rate to initiate groundwater recharge. As K_z increases, so must the Brooks and
368 Corey ϵ , limiting the value of unsaturated hydraulic conductivity and preventing the aquifer from
369 becoming inundated with excess water.

370 *3.3 Effects of lagged responses on aquifer usable lifespan*

371 These lagged responses to groundwater conservation lead to different estimates of the
372 degree to which conservation extends the usable aquifer lifetime. The lateral-flow-dominated
373 cases had an average extension of 15 years for a 20% pumping reduction and an average
374 extension of 25 years for a 30% reduction (Figure 7a, c). Results were similar for the recharge-
375 dominated cases, where the average extension was 12 years with a reduction in pumping of 20%
376 and 20 years for a pumping reduction of 30% (Figure 7b, d). Using the start of the initial SD-6
377 LEMA in 2013, the remaining usable lifetime can be quantified. For the recharge-dominated
378 cases, if no pumping reductions are applied, the water table will fall below eight meters of
379 saturated thickness (the minimum thickness capable of supporting irrigated agriculture (Butler et
380 al., 2020b) in 2047. If pumping is reduced by 20% or 30%, this usable expiration date changes to
381 2059 and 2067, respectively. In the lateral-flow-dominated cases, enacting no pumping
382 reductions sets the usable aquifer expiration date at 2045. With a 20% and 30% pumping
383 reduction, this date is extended to 2060 and 2070, respectively. The numbers found in this study
384 are within the envelope found by Butler et al. (2020b) who used a data-driven approach to
385 quantify the extension of usable lifetime under various exploratory scenarios. Our analysis
386 extends this previous work by quantifying the relative importance of lateral flow and recharge as
387 drivers of long-term change in net inflows.

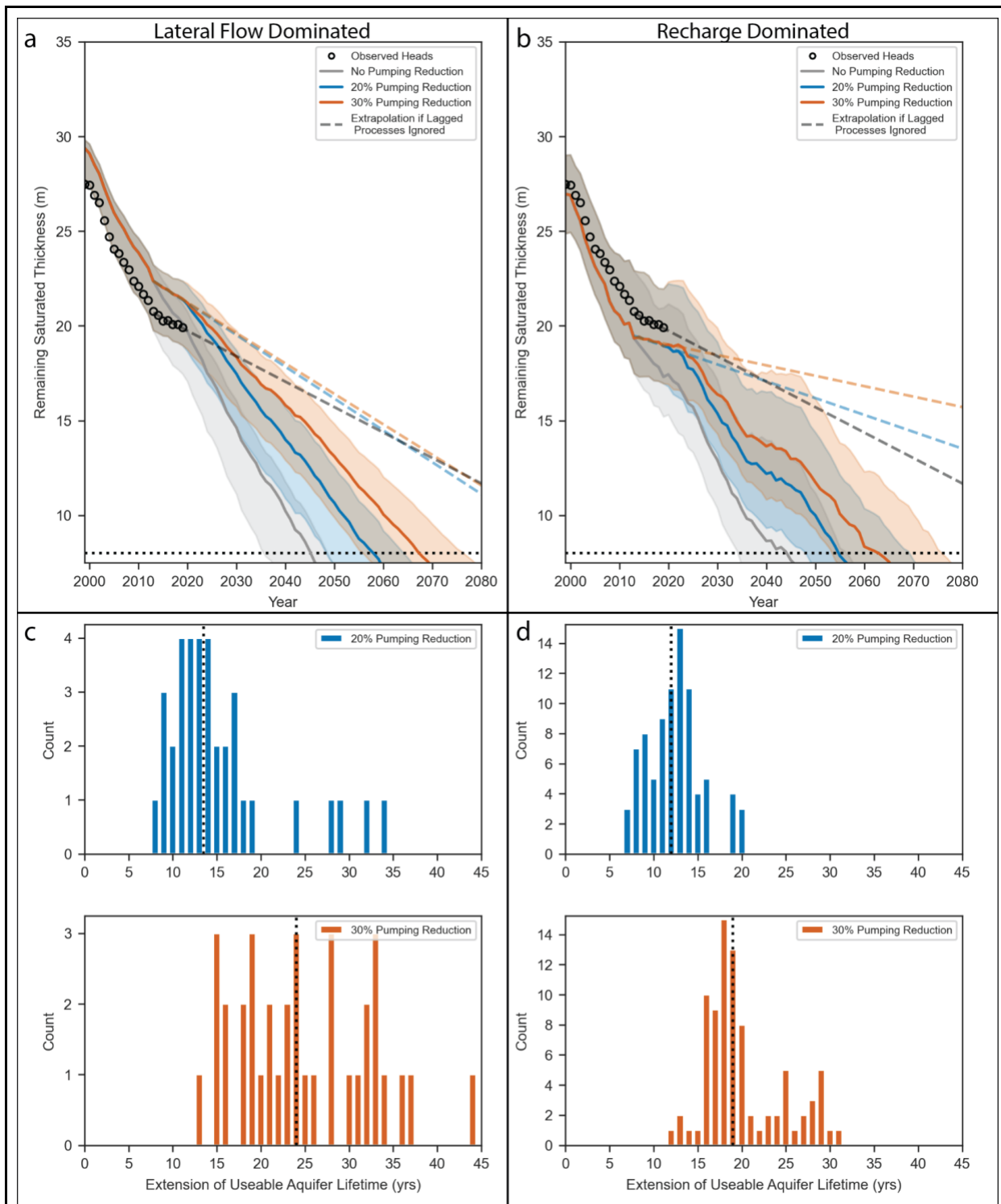


Figure 7: a) and b): Median simulated saturated thickness for the three pumping scenarios for a) lateral-flow-dominated and b) recharge-dominated cases. Dashed lines represent extrapolated remaining saturated thickness if the impact of lagged responses is ignored. The horizontal dotted line represents the minimum saturated thickness (eight meters) needed for large-scale

irrigated agriculture. c) and d): Median extension of usable lifetime (vertical black dotted line) and histogram of model outcomes for the 20% and 30% pumping reduction scenarios for c) lateral-flow-dominated and d) recharge-dominated cases. Shaded areas in panels a) and b) represent the interquartile range of the simulated projections.

388

389 In general, these results indicate that the effectiveness of groundwater conservation could
390 be overestimated if only using data from the period between initiation of pumping reductions and
391 the onset of the lagged responses. Using the observed heads from 2013 to 2019 and extrapolating
392 until the aquifer thickness drops below eight meters, the usable lifespan extends to 2107 (Figure
393 7a,b black dashed line). For the lateral flow-dominated cases, this value drops to 2098 for the
394 20% pumping reduction scenario and 2102 for the 30% pumping reduction scenario (Figure 7a,
395 blue and orange dashed lines). The recharge-dominated cases result in a much greater duration
396 with the usable lifetime extending to 2142 for the 20% pumping reduction case and 2220 for the
397 30% pumping reduction case (Figure 7b, blue and orange dashed lines). Using only the initial
398 appearance of pumping reduction effectiveness and ignoring the impacts of lagged responses
399 leads to drastically different interpretations of the effectiveness of these conservation methods.
400 The subsequent rebound in the water table decline rate dictates the long term effectiveness of
401 groundwater conservation strategies. Understanding the mechanisms that control these lagged
402 responses can manage stakeholder expectations and lead to the design of more effective
403 conservation strategies that can further extend the usable lifetime of stressed aquifers. For
404 example, as the effectiveness of initial conservation measures wanes and a return to increased
405 water table decline rates begin to be observed, Butler et al. (2020b) have shown that additional
406 pumping reductions can further extend usable aquifer lifetimes.

407

408 ***3.4 Implications of isolated conservation areas within heavily stressed regional aquifers***

409 Conservation strategies are most likely to be enacted in the most heavily stressed
410 aquifers. In the United States, these are located in the west where the doctrine of prior
411 appropriation, or colloquially “*first in time - first in right*”, is the guiding principle for water
412 rights (Johnson & DuMars, 1989). This has led to extensive litigation that will likely increase as
413 water resources are diminished through time (Griggs, 2013). We found that lateral flow out of
414 the conservation area (Figure 6) means that some of the water savings are transferred to non-
415 conservation areas (Figure 8), effectively subsidizing those outside the conservation area. As our
416 modeling setup is symmetric, the largest extension of usable lifetime occurs in the center of the
417 conservation area (values plotted in Figure 7) and decreases towards and across the boundary
418 between the conservation and non-conservation areas. This pattern is greater under the lateral
419 flow-dominated cases but also occurs in recharge-dominated cases due to the reduction-induced
420 gradient changes discussed above. The activities in the conservation area will affect the usable
421 aquifer lifetime in the nearby non-conservation area. Without any reductions in pumping, this
422 area achieves an extension of at least 5 years at distances of approximately 2 km from the
423 boundary for the 20% pumping reduction case and between 3.5 and 4 km for the 30% pumping
424 reduction case. Extensions of the usable aquifer lifetime at 7 km from the boundary range
425 between about 0.75 and 2 years. However, the magnitude of this effect is dependent on the
426 horizontal conductivity value. The lateral flow subsidy would also be smaller (relative to the
427 volume of water conserved within the conservation area) as the size of the conservation area
428 increases.

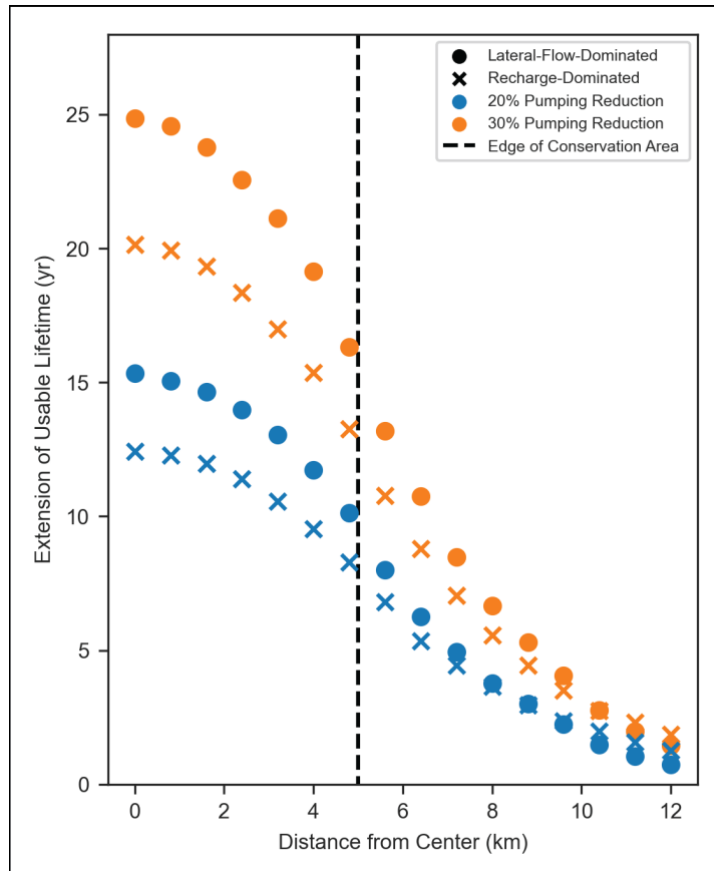


Figure 8: Average extension of usable aquifer lifetime for the lateral-flow-dominated (circles) and recharge-dominated (Xs) compared to distance from the center of the conservation area.

429

430 While our surrogate model simulations found net outflow across the LEMA boundary, in

431 practice many overexploited areas where groundwater conservation measures may be

432 implemented are closed basins and therefore this may manifest through other impacts such as a

433 reduction in cross-boundary inflows to the conservation area (Pauloo et al., 2021). In either case,

434 this indicates that the benefits of pumping reductions can extend beyond the boundaries of the

435 areas with groundwater conservation initiatives, with potential socio-political impacts. For

436 instance, if pumping reductions are implemented in trans-boundary aquifers, lagged responses

437 should be accounted for to ensure that water resources are shared equitably, not just within the

438 United States but across the globe (Callegary et al., 2018; Lee et al., 2018; Lipponen & Chilton,
439 2018; Sindico et al., 2018).

440 *3.5 Limitations and future research needs*

441 Although the modeling framework presented here represented the interannual and annual
442 dynamics of the observed natural system (Figure 5), there are several limitations to our approach
443 that may affect the results. First, aquifers are inherently complex, spatially heterogeneous, and
444 frequently lack sufficient observation data. Our analysis deliberately simplified this complexity
445 into a homogeneous surrogate model in order to isolate the lagged hydrological responses to
446 groundwater conservation, and therefore does not capture the intricacies of the natural world,
447 such as spatial changes in depth to bedrock, strata discontinuity, or incorporation of regional
448 groundwater gradients. Additionally, although Kansas has the most robust groundwater well
449 metering data across the United States (Foster et al., 2020; USDA National Agricultural
450 Statistics Service, 2019), the spatial distribution of wells used for pumping and observation data
451 is not captured in our study as we evenly distributed pumping across the conservation and non-
452 conservation areas to investigate average processes within the LEMA.

453 Second, the applied pumping and deep percolation rates are based on statistical
454 relationships using limited data. Pumping rates for the period from 1955 to 1992 are based on a
455 regression model while rates from 1993 to 2018 are based on observed data. Additionally, when
456 developing the projected pumping rates, we assumed that irrigation efficiency does not change,
457 which may not be the case as new technologies are adopted by the agricultural community.
458 Applied deep percolation rates were developed using ten years of modeled data and extrapolated
459 to fill the historical record, which may have resulted in deep percolation rates that are too high.
460 We also assumed that the east-to-west lateral inflows to the system are constant through time.

461 These issues point to a critical need to better monitor vertical fluxes of water in deep vadose
462 zones and lateral fluxes in aquifers to inform future modeling efforts and conservation program
463 evaluations.

464 Third, the use of the UZF package to simulate variably saturated flow is limited in several
465 aspects. If applied deep percolation rates are greater than the prescribed saturated hydraulic
466 conductivity, excess water is removed from the system, as low hydraulic conductivity conditions
467 typical of lateral-flow-dominated cases are limited not just by the rate at which water percolates
468 through the unsaturated zone, but also by the supply of water able to infiltrate into the root zone.
469 Applying heterogeneity to the model domain was not possible with the UZF package as it can
470 only be applied to one active layer, further simplifying the representation. We had attempted to
471 address this limitation by using another MODFLOW-based variably-saturated flow solution,
472 HYDRUS Package for MODFLOW (Beegum et al., 2018; Seo et al., 2007), which solves a 1-D
473 unsaturated Richards Equation for each cell column, but experienced both instability and
474 anomalous results that prevented its application here. Finally, all projection results are based on
475 randomly sampling the historical record of precipitation to generate time series for deep
476 percolation and pumping, which provides realistic daily meteorological dynamics but inherently
477 ignores climate change impacts and implications.

478 Although our modeling approach may disregard some locally important heterogeneity,
479 our objective was to analyze the major factors controlling the long-term effectiveness of
480 groundwater conservation initiatives. Our simplified surrogate modeling approach allows for the
481 fundamental processes to be investigated while removing the impact of site specific phenomena,
482 ultimately allowing for a more generalized understanding of system dynamics. Applying these
483 assumptions, we were able to investigate the interplay between hydraulic properties and

484 recharge, the long-term effectiveness of pumping reduction based groundwater conservation
485 strategies, and estimate the extension of the usable aquifer lifetime for both the lateral-flow- and
486 recharge-dominated cases.

487 **4. Conclusions**

488 In this study, we demonstrate that groundwater conservation strategies based on pumping
489 reductions are an effective method for conserving groundwater over a period of decades. Our
490 results indicate that there are two possible controlling mechanisms, lateral groundwater inflow
491 and recharge, that ultimately govern the long-term effectiveness of such conservation initiatives.
492 We found that larger reductions in pumping result in a longer extension of the usable aquifer
493 lifetime, and that this impact wanes toward the edges of the conservation area. However, we also
494 found that reductions in pumping result in a groundwater mound relative to the surroundings that
495 alters the regional hydraulic gradient, so that the benefits of groundwater conservation programs
496 may extend beyond the areas implementing conservation practices. These results show that
497 initial water table data might overestimate the long-term effectiveness of pumping reduction-
498 based groundwater conservation , and that a robust understanding of the local geology and
499 groundwater flow are imperative for designing resource conservation programs and
500 communicating their likely future path to the stakeholder community.

501 **Acknowledgments**

502 This work was supported, in part, by the United States Department of Agriculture (USDA) under
503 USDA-NIFA grant 2018-67003-27406 and subaward RC104693B, and the USDA and the
504 National Science Foundation (NSF) under USDA-NIFA/NSF-INFIEWS grant 2018-67003-27406
505 and subaward RC108063UK. Any opinions, findings, and conclusions or recommendations
506 expressed in this material are those of the authors and do not necessarily reflect the views of the

507 USDA or NSF. We would like to thank Geoff Bohling and Brownie Wilson for their help
508 procuring data and helpful comments. Data and code are available at
509 https://github.com/tomglose/SD6_Modeling_Project.git during the review process and will be
510 placed in a repository at the time of paper acceptance.

511

512 **References**

- 513 Aeschbach-Hertig, W., & Gleeson, T. (2012). Regional strategies for the accelerating global
514 problem of groundwater depletion. *Nature Geoscience*, *5*(12), 853–861.
515 <https://doi.org/10.1038/ngeo1617>
- 516 Ajaz, A., Datta, S., & Stoodley, S. (2020). High Plains Aquifer–State of Affairs of Irrigated
517 Agriculture and Role of Irrigation in the Sustainability Paradigm. *Sustainability*, *12*(9),
518 3714. <https://doi.org/10.3390/su12093714>
- 519 Asher, M. J., Croke, B. F. W., Jakeman, A. J., & Peeters, L. J. M. (2015). A review of surrogate
520 models and their application to groundwater modeling. *Water Resources Research*, *51*(8),
521 5957–5973. <https://doi.org/10.1002/2015WR016967>
- 522 Bailey, R. T., Morway, E. D., Niswonger, R. G., & Gates, T. K. (2013). Modeling Variably
523 Saturated Multispecies Reactive Groundwater Solute Transport with MODFLOW-UZF
524 and RT3D. *Groundwater*, *51*(5), 752–761. [https://doi.org/10.1111/j.1745-](https://doi.org/10.1111/j.1745-6584.2012.01009.x)
525 [6584.2012.01009.x](https://doi.org/10.1111/j.1745-6584.2012.01009.x)
- 526 Bakker, M., Post, V., Langevin, C. D., Hughes, J. D., White, J. T., Starn, J. J., & Fienen, M. N.
527 (2016). Scripting MODFLOW Model Development Using Python and FloPy.
528 *Groundwater*, *54*(5), 733–739. <https://doi.org/10.1111/gwat.12413>
- 529 Beegum, S., Šimůnek, J., Szymkiewicz, A., Sudheer, K. P., & Nambi, I. M. (2018). Updating the
530 Coupling Algorithm between HYDRUS and MODFLOW in the HYDRUS Package for
531 MODFLOW. *Vadose Zone Journal*, *17*(1), 180034.
532 <https://doi.org/10.2136/vzj2018.02.0034>
- 533 Beven, K. (2006). A manifesto for the equifinality thesis. *The Model Parameter Estimation*
534 *Experiment*, *320*(1), 18–36. <https://doi.org/10.1016/j.jhydrol.2005.07.007>

535 Bierkens, M. F. P., & Wada, Y. (2019). Non-renewable groundwater use and groundwater
536 depletion: a review. *Environmental Research Letters*, *14*(6), 063002.
537 <https://doi.org/10.1088/1748-9326/ab1a5f>

538 Brooks, R. H., & Corey, A. T. (1966). Properties of porous media affecting fluid flow. *Journal of*
539 *the Irrigation and Drainage Division*, *92*(2), 61–90.

540 Butler, J. J., Jr., Whittemore, D. O., Wilson, B. B., & Bohling, G. C. (2016). A new approach for
541 assessing the future of aquifers supporting irrigated agriculture. *Geophysical Research*
542 *Letters*, *43*(5), 2004–2010. <https://doi.org/10.1002/2016GL067879>

543 Butler, J. J., Jr., Whittemore, D. O., Reboulet, E. C., Knobbe, S., Wilson, B. B., & Bohling, G. C.
544 (2019). High Plains aquifer index well program: 2019 annual report.

545 Butler, J. J., Jr., Bohling, G. C., Whittemore, D. O., & Wilson, B. B. (2020a). A roadblock on the
546 path to aquifer sustainability: underestimating the impact of pumping reductions.
547 *Environmental Research Letters*, *15*(1), 014003. [https://doi.org/10.1088/1748-](https://doi.org/10.1088/1748-9326/ab6002)
548 [9326/ab6002](https://doi.org/10.1088/1748-9326/ab6002)

549 Butler, J. J., Jr., Bohling, G. C., Whittemore, D. O., & Wilson, B. B. (2020b). Charting Pathways
550 Toward Sustainability for Aquifers Supporting Irrigated Agriculture. *Water Resources*
551 *Research*, *56*(10), e2020WR027961. <https://doi.org/10.1029/2020WR027961>

552 Callegary, J. B., Megdal, S. B., Tapia Villaseñor, E. M., Petersen-Perlman, J. D., Minjárez Sosa,
553 I., Monreal, R., et al. (2018). Findings and lessons learned from the assessment of the
554 Mexico-United States transboundary San Pedro and Santa Cruz aquifers: The utility of
555 social science in applied hydrologic research. *Special Issue on International Shared*
556 *Aquifer Resources Assessment and Management*, *20*, 60–73.
557 <https://doi.org/10.1016/j.ejrh.2018.08.002>

558 Castilla-Rho, J. C., Rojas, R., Andersen, M. S., Holley, C., & Mariethoz, G. (2019). Sustainable
559 groundwater management: How long and what will it take? *Global Environmental*
560 *Change*, 58, 101972. <https://doi.org/10.1016/j.gloenvcha.2019.101972>

561 Deines, J. M., Kendall, A. D., Butler, J. J., Jr., & Hyndman, D. W. (2019). Quantifying irrigation
562 adaptation strategies in response to stakeholder-driven groundwater management in the
563 US High Plains Aquifer. *Environmental Research Letters*, 14, 044014.
564 <https://doi.org/10.1088/1748-9326/aafe39>

565 Deines, J. M., Schipanski, M. E., Golden, B., Zipper, S. C., Nozari, S., Rottler, C., et al. (2020).
566 Transitions from irrigated to dryland agriculture in the Ogallala Aquifer: Land use
567 suitability and regional economic impacts. *Agricultural Water Management*, 233,
568 106061. <https://doi.org/10.1016/j.agwat.2020.106061>

569 Deines, J. M., Kendall, A. D., Butler, J. J., Jr., Basso, B., & Hyndman, D. W. (2021). Combining
570 Remote Sensing and Crop Models to Assess the Sustainability of Stakeholder-Driven
571 Groundwater Management in the US High Plains Aquifer. *Water Resources Research*,
572 e2020WR027756. <https://doi.org/10.1029/2020WR027756>

573 DeSimone, L. A., McMahon, P. B., & Rosen, M. R. (2015). *The quality of our Nation's waters:*
574 *Water quality in principal aquifers of the United States, 1991-2010* (Report No. 1360) (p.
575 161). Reston, VA. <https://doi.org/10.3133/cir1360>

576 Dieter, C. A., Maupin, M. A., Caldwell, R. R., Harris, M. A., Ivahnenko, T. I., Lovelace, J. K., et
577 al. (2018). *Estimated use of water in the United States in 2015* (Report No. 1441) (p. 76).
578 Reston, VA. <https://doi.org/10.3133/cir1441>

579 Doherty, J. (2015). *Calibration and uncertainty analysis for complex environmental models*.
580 Watermark Numerical Computing Brisbane, Australia.

581 Foster, T., Brozović, N., & Butler, A. P. (2017). Effects of initial aquifer conditions on economic
582 benefits from groundwater conservation. *Water Resources Research*, 53(1), 744–762.
583 <https://doi.org/10.1002/2016WR019365>

584 Foster, T., Mieno, T., & Brozović, N. (2020). Satellite-Based Monitoring of Irrigation Water
585 Use: Assessing Measurement Errors and Their Implications for Agricultural Water
586 Management Policy. *Water Resources Research*, 56(11), e2020WR028378.
587 <https://doi.org/10.1029/2020WR028378>

588 Fross, D., Sophocleous, M. A., Wilson, B. B., & Butler, J. J., Jr. (2012). Kansas High Plains
589 Aquifer Atlas, Kansas Geological Survey. Retrieved from
590 http://www.kgs.ku.edu/HighPlains/HPA_Atlas/index.html

591 Gleeson, T., Cuthbert, M., Ferguson, G., & Perrone, D. (2020). Global Groundwater
592 Sustainability, Resources, and Systems in the Anthropocene. *Annual Review of Earth and*
593 *Planetary Sciences*, 48(1), 431–463. [https://doi.org/10.1146/annurev-earth-071719-](https://doi.org/10.1146/annurev-earth-071719-055251)
594 [055251](https://doi.org/10.1146/annurev-earth-071719-055251)

595 Golden, B. (2018). *Monitoring the Impacts of Sheridan County 6 Local Enhanced*
596 *Management Area: Final Report for 2013 – 2017*. Manhattan, KS. Retrieved from
597 [https://agriculture.ks.gov/docs/default-source/dwr-water-appropriation-](https://agriculture.ks.gov/docs/default-source/dwr-water-appropriation-documents/sheridancounty6_lemma_goldenreport_2013-2017.pdf?sfvrsn=dac48ac1_0)
598 [documents/sheridancounty6_lemma_goldenreport_2013-2017.pdf?sfvrsn=dac48ac1_0](https://agriculture.ks.gov/docs/default-source/dwr-water-appropriation-documents/sheridancounty6_lemma_goldenreport_2013-2017.pdf?sfvrsn=dac48ac1_0)

599 Griggs, B. W. (2013). Beyond drought: Water rights in the age of permanent depletion. *U. Kan.*
600 *l. Rev.*, 62, 1263.

601 Gurdak, J. J., Walvoord, M. A., & McMahon, P. B. (2008). Susceptibility to Enhanced Chemical
602 Migration from Depression-Focused Preferential Flow, High Plains Aquifer. *Vadose*
603 *Zone Journal*, 7(4), 1218–1230. <https://doi.org/10.2136/vzj2007.0145>

604 Hansen, C. V. (1991). *Estimates of freshwater storage and potential natural recharge for*
605 *principal aquifers in Kansas* (Report No. 87-4230). <https://doi.org/10.3133/wri874230>

606 Hou, X., Wang, S., Jin, X., Li, M., Lv, M., & Feng, W. (2020). Using an ETWatch (RS)-UZP-
607 MODFLOW Coupled Model to Optimize Joint Use of Transferred Water and Local
608 Water Sources in a Saline Water Area of the North China Plain. *Water*, 12(12), 3361.

609 Hu, Y., Moiwo, J. P., Yang, Y., Han, S., & Yang, Y. (2010). Agricultural water-saving and
610 sustainable groundwater management in Shijiazhuang Irrigation District, North China
611 Plain. *Journal of Hydrology*, 393(3), 219–232.
612 <https://doi.org/10.1016/j.jhydrol.2010.08.017>

613 Hunt, R. J., Prudic, D. E., Walker, J. F., & Anderson, M. P. (2008). Importance of Unsaturated
614 Zone Flow for Simulating Recharge in a Humid Climate. *Groundwater*, 46(4), 551–560.
615 <https://doi.org/10.1111/j.1745-6584.2007.00427.x>

616 Johnson, N. K., & DuMars, C. T. (1989). A survey of the evolution of western water law in
617 response to changing economic and public interest demands. *Natural Resources Journal*,
618 29(2), 347–387.

619 Kansas Department of Agriculture. (2013). Order of designation approving the Sheridan 6 Local
620 Enhanced Management Area within Groundwater Management District No. 4. Retrieved
621 from
622 <https://sftp.kda.ks.gov:4443/LEMAs/SD6/LEMA.SD6.OrderOfDesignation.20130417.pdf>
623 f

624 Kansas Department of Agriculture. (2018). Order of designation regarding the Groundwater
625 Management District No. 4 District Wide Local Enhanced Management Plan. Retrieved
626 from <https://agriculture.ks.gov/docs/default-source/dwr-water-appropriation->

627 documents/gmd4_lemma_orderofdesignation.pdf?sfvrsn=30e981c1_4

628 Kansas Department of Agriculture. (2021). Order of designation regarding the Management Plan
629 for the Wichita County Local Enhanced Management Area. Retrieved from
630 [https://agriculture.ks.gov/docs/default-source/dwr-water-appropriation-documents/whc-](https://agriculture.ks.gov/docs/default-source/dwr-water-appropriation-documents/whc-lemma-order-of-designation---final.pdf?sfvrsn=60d690c1_0)
631 [lemma-order-of-designation---final.pdf?sfvrsn=60d690c1_0](https://agriculture.ks.gov/docs/default-source/dwr-water-appropriation-documents/whc-lemma-order-of-designation---final.pdf?sfvrsn=60d690c1_0)

632 Kansas Statutes Annotated 82a-1041. (2012). Local enhanced management areas; establishment
633 procedures; duties of chief engineer; hearing; notice; orders; review. Retrieved from
634 http://www.ksrevisor.org/statutes/chapters/ch82a/082a_010_0041.html

635 Katz, B. S., Stotler, R. L., Hirmas, D., Ludvigson, G., Smith, J. J., & Whittemore, D. O. (2016).
636 Geochemical Recharge Estimation and the Effects of a Declining Water Table. *Vadose*
637 *Zone Journal*, 15(vzj2016.04.0031). <https://doi.org/10.2136/vzj2016.04.0031>

638 Kennedy, J., Ferré, T. P. A., & Creutzfeldt, B. (2016). Time-lapse gravity data for monitoring
639 and modeling artificial recharge through a thick unsaturated zone. *Water Resources*
640 *Research*, 52(9), 7244–7261. <https://doi.org/10.1002/2016WR018770>

641 Kling, H., Fuchs, M., & Paulin, M. (2012). Runoff conditions in the upper Danube basin under
642 an ensemble of climate change scenarios. *Journal of Hydrology*, 424–425, 264–277.
643 <https://doi.org/10.1016/j.jhydrol.2012.01.011>

644 Konikow, L. F., & Bredehoeft, J. D. (1992). Ground-water models cannot be validated.
645 *Validation of Geo-Hydrological Models Part 1*, 15(1), 75–83.
646 [https://doi.org/10.1016/0309-1708\(92\)90033-X](https://doi.org/10.1016/0309-1708(92)90033-X)

647 Lee, E., Jayakumar, R., Shrestha, S., & Han, Z. (2018). Assessment of transboundary aquifer
648 resources in Asia: Status and progress towards sustainable groundwater management.
649 *Special Issue on International Shared Aquifer Resources Assessment and Management*,

650 20, 103–115. <https://doi.org/10.1016/j.ejrh.2018.01.004>

651 Lin, X., Harrington, J., Ciampitti, I., Gowda, P., Brown, D., & Kisekka, I. (2017). Kansas Trends
652 and Changes in Temperature, Precipitation, Drought, and Frost-Free Days from the 1890s
653 to 2015. *Journal of Contemporary Water Research & Education*, 162(1), 18–30.
654 <https://doi.org/10.1111/j.1936-704X.2017.03257.x>

655 Lipponen, A., & Chilton, J. (2018). Development of cooperation on managing transboundary
656 groundwaters in the pan-European region: The role of international frameworks and joint
657 assessments. *Special Issue on International Shared Aquifer Resources Assessment and*
658 *Management*, 20, 145–157. <https://doi.org/10.1016/j.ejrh.2018.05.001>

659 McKay, M. D., Beckman, R. J., & Conover, W. J. (1979). Comparison of Three Methods for
660 Selecting Values of Input Variables in the Analysis of Output from a Computer Code.
661 *Technometrics*, 21(2), 239–245. <https://doi.org/10.1080/00401706.1979.10489755>

662 McMahon, P. B., Dennehy, K. F., Bruce, B. W., Böhlke, J. K., Michel, R. L., Gurdak, J. J., &
663 Hurlbut, D. B. (2006). Storage and transit time of chemicals in thick unsaturated zones
664 under rangeland and irrigated cropland, High Plains, United States. *Water Resources*
665 *Research*, 42(3). <https://doi.org/10.1029/2005WR004417>

666 Morway, E. D., Niswonger, R. G., Langevin, C. D., Bailey, R. T., & Healy, R. W. (2013).
667 Modeling Variably Saturated Subsurface Solute Transport with MODFLOW-UZF and
668 MT3DMS. *Groundwater*, 51(2), 237–251. <https://doi.org/10.1111/j.1745->
669 [6584.2012.00971.x](https://doi.org/10.1111/j.1745-6584.2012.00971.x)

670 Nazarieh, F., Ansari, H., Ziaei, A. N., Izady, A., Davari, K., & Brunner, P. (2018). Spatial and
671 temporal dynamics of deep percolation, lag time and recharge in an irrigated semi-arid
672 region. *Hydrogeology Journal*, 26(7), 2507–2520. <https://doi.org/10.1007/s10040-018->

673 1789-z

674 Niswonger, R. G., & Prudic, D. E. (2009). Comment on “Evaluating Interactions between
675 Groundwater and Vadose Zone Using the HYDRUS-Based Flow Package for
676 MODFLOW” by Navin Kumar C. Twarakavi, Jirka Šimůnek, and Sophia Seo. *Vadose
677 Zone Journal*, 8(3), 818–819. <https://doi.org/10.2136/vzj2008.0155>

678 Niswonger, R. G., Prudic, D. E., & Regan, R. S. (2006). *Documentation of the Unsaturated-Zone
679 Flow (UZFI) Package for modeling Unsaturated Flow Between the Land Surface and the
680 Water Table with MODFLOW-2005* (Report No. 6-A19). <https://doi.org/10.3133/tm6A19>

681 Pauloo, R. A., Fogg, G. E., Guo, Z., & Harter, T. (2021). Anthropogenic basin closure and
682 groundwater salinization (ABCSAL). *Journal of Hydrology*, 593, 125787.
683 <https://doi.org/10.1016/j.jhydrol.2020.125787>

684 Pfeiffer, L., & Lin, C.-Y. C. (2010). The effect of irrigation technology on groundwater use.
685 *Choices*, 25(3), 1–6.

686 Poeter, E. P., & Hill, M. C. (1999). UCODE, a computer code for universal inverse modeling.
687 *Computers & Geosciences*, 25(4), 457–462.

688 Razavi, S., Tolson, B. A., & Burn, D. H. (2012). Review of surrogate modeling in water
689 resources. *Water Resources Research*, 48(7). <https://doi.org/10.1029/2011WR011527>

690 Rogers, D. H., & Lamm, F. R. (2012). Kansas irrigation trends. Presented at the Proceedings of
691 the 24th Annual Central Plains Irrigation Conference, Colby, Kansas, February 21-22,
692 2012, Central Plains Irrigation Association.

693 Scanlon, B. R., Keese, K. E., Flint, A. L., Flint, L. E., Gaye, C. B., Edmunds, W. M., &
694 Simmers, I. (2006). Global synthesis of groundwater recharge in semiarid and arid
695 regions. *Hydrological Processes*, 20(15), 3335–3370. <https://doi.org/10.1002/hyp.6335>

696 Scanlon, B. R., Faunt, C. C., Longuevergne, L., Reedy, R. C., Alley, W. M., McGuire, V. L., &
697 McMahon, P. B. (2012). Groundwater depletion and sustainability of irrigation in the US
698 High Plains and Central Valley. *Proceedings of the National Academy of Sciences*,
699 *109*(24), 9320–9325. <https://doi.org/10.1073/pnas.1200311109>

700 Seo, H. S., Simunek, J., & Poeter, E. P. (2007). Documentation of the hydrus package for
701 modflow-2000, the us geological survey modular ground-water model. *IGWMC-*
702 *International Ground Water Modeling Center*.

703 Sindico, F., Hirata, R., & Manganelli, A. (2018). The Guarani Aquifer System: From a Beacon
704 of hope to a question mark in the governance of transboundary aquifers. *Special Issue on*
705 *International Shared Aquifer Resources Assessment and Management*, *20*, 49–59.
706 <https://doi.org/10.1016/j.ejrh.2018.04.008>

707 Smith, R. (1983). Approximate soil water movement by kinematic characteristics. *Soil Science*
708 *Society of America Journal*, *47*(1), 3–8.

709 Smith, R., & Hebbert, R. H. B. (1983). Mathematical simulation of interdependent surface and
710 subsurface hydrologic processes. *Water Resources Research*, *19*(4), 987–1001.
711 <https://doi.org/10.1029/WR019i004p00987>

712 USDA National Agricultural Statistics Service. (2019). 2018 Irrigation and water management
713 survey, 3. Retrieved from
714 [https://www.nass.usda.gov/Publications/AgCensus/2017/Online_Resources/Farm_and_R](https://www.nass.usda.gov/Publications/AgCensus/2017/Online_Resources/Farm_and_Ranch_Irrigation_Survey/fris.pdf)
715 [anch_Irrigation_Survey/fris.pdf](https://www.nass.usda.gov/Publications/AgCensus/2017/Online_Resources/Farm_and_Ranch_Irrigation_Survey/fris.pdf)

716 Voss, C. I. (2011a). Editor’s message: Groundwater modeling fantasies —part 1, adrift in the
717 details. *Hydrogeology Journal*, *19*(7), 1281–1284. [https://doi.org/10.1007/s10040-011-](https://doi.org/10.1007/s10040-011-0789-z)
718 [0789-z](https://doi.org/10.1007/s10040-011-0789-z)

719 Voss, C. I. (2011b). Editor's message: Groundwater modeling fantasies—part 2, down to earth.
720 *Hydrogeology Journal*, 19(8), 1455–1458. <https://doi.org/10.1007/s10040-011-0790-6>

721 Whittlemore, D. O., Butler, J. J., Jr., & Wilson, B. B. (2018). Status of the High Plains Aquifer in
722 Kansas. *Kansas Geological Survey Technical Series*, 22. Retrieved from
723 www.kgs.ku.edu/Publications/Bulletins/TS22/index.html

724 Zell, W. O., & Sanford, W. E. (2020). Calibrated Simulation of the Long-Term Average Surficial
725 Groundwater System and Derived Spatial Distributions of its Characteristics for the
726 Contiguous United States. *Water Resources Research*, 56(8), e2019WR026724.
727 <https://doi.org/10.1029/2019WR026724>

728 Zipper, S. C., Lamontagne-Hallé, P., McKenzie, J. M., & Rocha, A. V. (2018). Groundwater
729 Controls on Postfire Permafrost Thaw: Water and Energy Balance Effects. *Journal of*
730 *Geophysical Research: Earth Surface*, 123(10), 2677–2694.
731 <https://doi.org/10.1029/2018JF004611>

732 Zipper, S. C., Gleeson, T., Kerr, B., Howard, J. K., Rohde, M. M., Carah, J., & Zimmerman, J.
733 (2019). Rapid and Accurate Estimates of Streamflow Depletion Caused by Groundwater
734 Pumping Using Analytical Depletion Functions. *Water Resources Research*, 55(7), 5807–
735 5829. <https://doi.org/10.1029/2018WR024403>

Supplemental Information

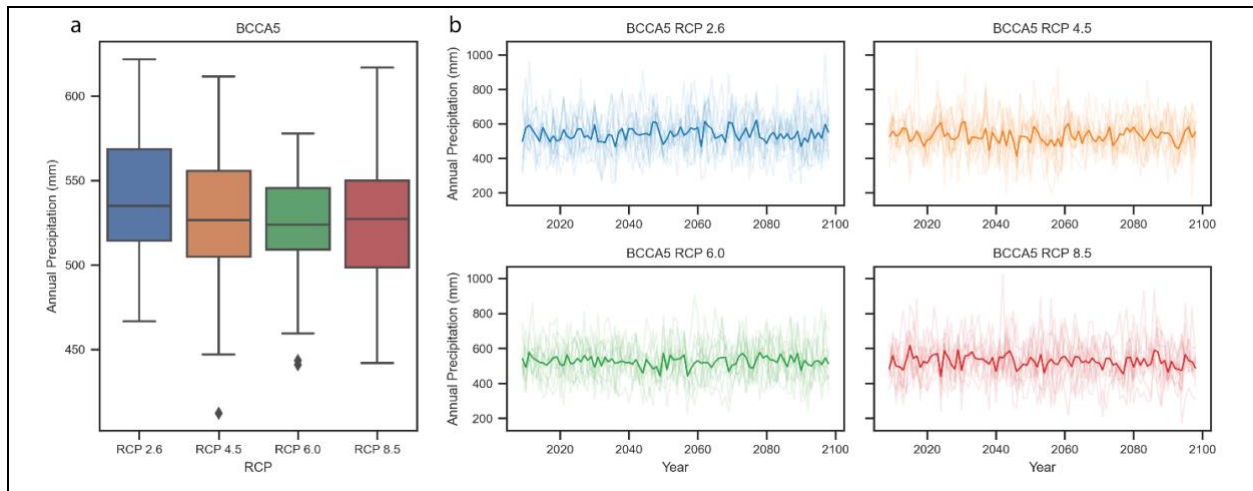


Figure S1: We used aggregated daily bias correction constructed analogs (BCCAs) for precipitation data from downscaled Coupled Model Intercomparison Project 5 (CMIP5) data in the area of the Sheridan-6 Local Enhanced Management Area to assess if there were any long-term trends in precipitation that needed to be considered. From the a.) boxplot displaying the ensemble mean and the b.) individual time series (lighter color) and ensemble mean (dark line) for each representative concentration pathway it is clear that there are no long-term trends in forecasted precipitation for this area.